Chemical Engineering Journal 152 (2009) 242–250

Contents lists available at ScienceDirect

Chemical Engineering Journal

journal homepage: www.elsevier.com/locate/cej

Kinetics of the catalytic isomerization and disproportionation of rosin over carbon-supported palladium

Linlin Wang, Xiaopeng Chen, Jiezhen Liang, Yueyuan Chen, Xiaodong Pu, Zhangfa Tong*

School of Chemistry and Chemical Engineering, Guangxi University, Nanning 530004, PR China

ARTICLE INFO

Article history:
Received 25 October 2008
Received in revised form 10 April 2009
Accepted 21 April 2009

Keywords:
Palladium/carbon
Rosin
Isomerization
Disproportionation
Kinetics

ABSTRACT

The kinetics of the catalytic isomerization and disproportionation of rosin over a Pd/C catalyst was investigated, using a novel experimental setup with a double-tier paddle agitator and specially designed sampling system, in No. 200 solvent oil and under a nitrogen atmosphere. The catalyst was characterized by scanning electron microscopy (SEM), X-ray powder diffraction (XRD) and nitrogen physisorption. Kinetic experiments, designed to eliminate mass transfer effects, were carried out at temperatures ranging from 483 to 533 K by gas chromatographic analysis of samples that were withdrawn at different intervals. A kinetic model for catalytic isomerization and disproportionation of rosin over a Pd/C catalyst was proposed, and the various activation energies were determined for the isomerization of neoabietic acid to abietic acid (156.14 kJ mol^{-1}), the isomerization of palustric acid to abietic acid (78.80 kJ mol^{-1}), the dehydrogenation of abietic acid to dehydroabietic acid (108.56 kJ mol^{-1}), the hydrogenation of abietic acid to hydrogenated abietic-type resin acids (105.75 kJ mol^{-1}) and the hydrogenation of pimarenoic acid-type resin acids to hydrogenated pimarenoic acid-type resin acids (97.35 kJ mol^{-1}). The results of the kinetic model agreed well with experimental observations within the initial experimental range and successfully predicted the concentration distribution of the products outside that range at 543 K.

1. Introduction

Rosin is a solid resinous mass naturally obtained from the oleoresin of the pine tree. It is composed mostly of rosin acids and some neutral matter. Approximately 90% of the rosin acids are of the abietic-type resin acids with conjugated double bonds and a single carboxylic group; e.g., abietic acid, palustric acid and neoabietic acid. The other 10% are the closely related pimaric-type resin acids with non-conjugated double bonds [1]. These have the typical formula $C_{19}H_{29}COOH$. The rosin can be modified to "disproportionated rosin" via a catalytic disproportionation reaction since the abietic-type resin acids contain chemically reactive conjugated double bonds. Disproportionated rosin is characterized by good oxidation resistance, low brittleness, high thermal stability and light color. Consequently, it has many important commercial uses; e.g., (i) as an emulsifier in the production of styrene–butadiene rubber, ABS resin and chloroprene rubber; (ii) as a raw material in the synthesis of rosin nitrile and (iii) as an intermediate in the synthesis of water soluble pressure-sensitive adhesives, printing inks, organic pigments, etc.

Furthermore, a series of recent studies have shown that dehydroabietic acid, the main constituent of disproportionated rosin, has additional possibly commercially important properties. For example, it has been reported that the amide derivatives of dehydroabietic acid possess effective blood serum cholesterol-reducing and anti-arteriosclerotic properties [2]. Also, Fonseca et al. [3] synthesized benzimidazoles, quinoxalines and indoles from dehydroabietic acid, which possess in vitro activity against several RNA and DNA viruses. Tapia et al. [4] have obtained a novel derivative of dehydroabietic acid, 1β-hydroxydehydroabietic acid, which has been shown to have interesting antimicrobial activity. Piispanen et al. [5] have also synthesized a new surfactant from dehydroabietic acid.

The disproportionation reaction of rosin is generally understood as an exchange of hydrogen between molecules of resin acids, whereby some resin acids are dehydrogenated and others hydrogenated [6]. Moreover, abietic-type resin acids can easily isomerize with the action of heat [7]. Because of the steric effects of the tricyclic skeleton structure of abietic acid and the high viscosity of fused rosin solution, the disproportionation reaction is usually carried out at high temperatures (523–563 K) in the presence of any of a variety of catalysts; e.g., strong mineral acid, iodine, sulfur, sulfur dioxide, selenium, Raney nickel and palladium on charcoal (Pd/C) [8–12]. The Pd/C has been regarded as the best catalyst for the disproportionation reaction of rosin. Therefore, a study of the reaction kinetics is especially valuable.

Several investigations have studied the conversion of various resin acids during rosin disproportionation [1,6,13], but there are

* Corresponding author. Tel.: +86 771 3233728; fax: +86 771 3233718.
E-mail address: bioche@gxu.edu.cn (Z.-F. Tong).

1385-8947/$ – see front matter © 2009 Elsevier B.V. All rights reserved.
doi:10.1016/j.cej.2009.04.052

few reports on kinetics of these reactions. Song et al. [6] reported on the composition change of resin acid during the disproportionation of American gum rosin over Pd/C catalyst at 543 K in a three neck round-bottom flask. The principal product was dehydroabietic acid with a small amount of dihydroabietic acids; the pimaric resin acids were readily hydrogenated. Song and Liang [14] described the change of resin acid composition as a function of time during disproportionation of Chinese gum rosin on Pd/C catalyst at 543 K in a three neck round-bottom flask. Dehydroabietic acid was formed as the main product, with relatively small amounts of dihydroabietic and tetrahydroabietic acids. The disproportionation conversion and yield from *P. massoniana* rosin were higher than that from *P. elliottii* rosin, given the same reaction time and conditions. However, no specific report has been published on the reaction kinetics for the catalytic disproportionation of rosin. We believe it is important to obtain detailed data for the reaction kinetics in order to design and optimize the reaction process.

Accordingly, the present paper focuses on the reaction kinetics for the catalytic disproportionation of rosin. A novel experimental setup, designed with an agitator for this liquid–solid reaction and equipped with a special sampling device, was used to study the kinetics of disproportionation at high temperature over a Pd/C catalyst. A kinetic model for the catalytic isomerization and disproportionation of rosin over Pd/C catalyst was proposed, and the kinetic parameters were estimated after eliminating internal and external diffusion effects.

2. Experimental

2.1. Materials

Gum rosin from *P. massoniana* pine tree was obtained from Guangxi Wuzhou Pine Chemicals Ltd., China. Its softening point is 348 K and acid number is 165 mg KOH/g.

No. 200 industrial grade solvent oil was obtained from Sinopec Maoming Refining & Chemical Co., Ltd., China. The solvent gasoline is composed mostly of alkane (C_4–C_{11}) and has the following properties: (i) density (at 20 °C): 767.3 kg/m^3; (ii) appearance: transparent, free of suspended matter, and insoluble in water; (iii) flash point (closed-cup): 42 °C; (iv) aromatic content: 14.58%; (v) distillation range: 140 (initial boiling point)–200 °C (98% distillate).

2.2. Catalyst

The Pd/C catalyst was prepared from palladium chloride (Shanghai Xingao Chemical Reagent Co., Ltd., China; palladium content ≥59% by weight) by the conventional method [15,16]. In summary, an aqueous solution of $PdCl_2$ in deionized water (hydrochloric acid was used to dissolve the $PdCl_2$) was rapidly added to the finely divided activated carbon. The slurry was stirred for 2 h at 303 K, then kept overnight and then mixed with sodium hydroxide solution to precipitate palladium as a hydroxide, which was stirred again and heated at 333 K for 1 h. After settling, the precipitate was filtered and washed. Excess formaldehyde was then added to the material in order to ensure complete reduction. Following further heating at 353 K for 1 h, the material was cooled, filtered, washed (until complete elimination of Cl^- ions) and dried. All of the Pd/C catalysts used in this experiment were taken from the same preparation batch.

The specific surface area (BET), total pore volume and average pore diameter were measured by nitrogen adsorption at 77 K in a Quantachrome NOVA 1200 instrument. The mean particle size distribution of the catalyst was measured with a Malvern Marstersizer. The morphology of the catalyst was observed by the Hitachi S-3400N scanning electron microscopy (SEM), using an acceleration voltage was 25 kV. The SEM–energy-dispersive X-ray system (EDS) analysis was obtained on an S-3400N scanning electron microscope, coupled to EDAX-Genesis energy-dispersive X-ray system, operated at 25 keV. Powder X-ray diffraction (XRD) was performed with a D/MAX2500 X-ray diffraction instrument, using Cu Kα at 40 kV and 200 mA, while scanning the sample over a Bragg angle (2θ) from 10° to 90°.

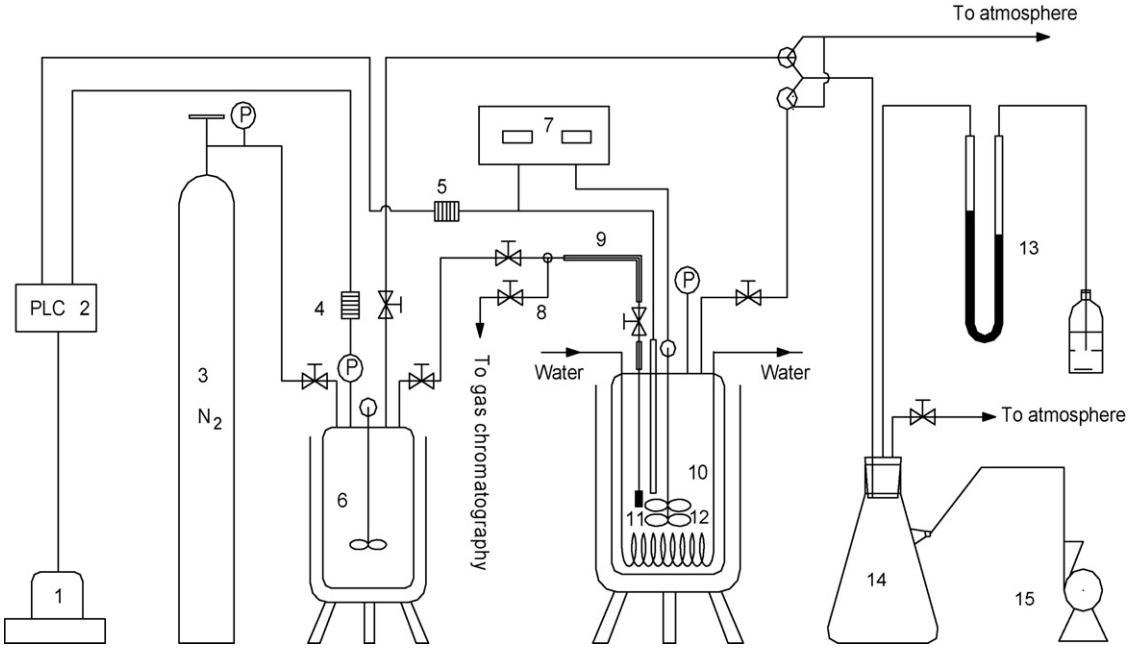

Fig. 1. Schematic diagram of the experimental setup. (1) Computer data collection system; (2) programmable logic controller; (3) nitrogen tank; (4) pressure transducer; (5) temperature transducer; (6) gauging pot; (7) temperature and stir control circuit; (8) sampling cell; (9) thermal retardation equipment of sampling; (10) reactor; (11) sampler; (12) double-tier paddle agitator; (13) mercury U-tube manometer; (14) pressure stabilization flask; (15) vacuum pump.

2.3. Experimental setup and procedure

2.3.1. Experimental setup and procedure of catalytic disproportionation

The experiments were performed in an agitated 2-L stainless steel batch reactor (Dalian Tongchan Autoclave Vessel Manufacturing Co., Ltd., China), whose design pressure is 20.0 MPa and design temperature is 623 K. The reactor was electrically heated with 1.5 kW heating power source. The pressure in the reactor was measured by a PMP731 pressure transducer (Matsushita Electric Works, Ltd., Japan), and the temperature by an EA-2 thermocouple (Dalian Tongchan Autoclave Vessel Manufacturing Co., Ltd., China). The results can be either read at the operation site, or transmitted to a computer for further analysis. A double-tier paddle agitator was used to increase the effect of the mass transfer between the liquid and solid systems. A schematic of the catalytic rosin disproportionation system is shown in Fig. 1.

Disproportionation runs were started by charging the reactor with 420 g of rosin (particle granularity ≤10 mm), 280 g of No. 200 solvent oil and 0.42 g of Pd/C catalyst. The reactor was then closed and sealed. The air was pumped out of the reactor to an absolute pressure of about 0.003 MPa, followed by charging with N_2 to a pressure at 0.5 MPa that was maintained for 15 min. Next, the N_2 was pumped out, and then the system was re-filled with N_2 to a pressure of 0.3 MPa. This evacuate-and-re-fill procedure was repeated twice more. Subsequently, the reactor was filled with N_2 to a pressure of 0.5 MPa. Then, the stirring and heating of the reactor began. The initial stirring speed was 50 rpm, which was increased to 500 rpm when the prescribed temperature was reached. As discussed in the following section, samples were withdrawn at predetermined reaction times for gas chromatography analysis. The present investigation was carried out at temperatures of 483, 493, 503, 513, 523 and 533 K.

2.3.2. Sampling system and method

In order to study the change in composition with time, the changes of the concentrations of reactants and products were followed over time by withdrawing samples during the course of reaction. Since the rosin liquid with high viscosity has a tendency to crystallize, special sampling system was used to address the problem of sampling a system under pressure and high temperature. Specifically, a sampling tube extending almost to the bottom of the reactor permitted the withdrawal of samples at frequent specified intervals. A stainless steel filter with diameter less than 10 μm was fixed onto the bottom of the sampling tube in order to prevent catalyst particles from being withdrawn with the liquid. Further, the stainless steel sampling tube (diameter 3 mm) outside the reactor was heated to prevent the rosin liquid from solidifying.

During the sampling operation, the T-valve in the sampling system was opened, and the tube was connected to the reaction system. Samples were withdrawn at predetermined reaction times for gas chromatographic analysis. Since the concentrations of the products in the reaction changed rapidly at the beginning of the reaction, samples of 0.5 cm^3 were taken approximately every 2 min during the first 5 min of the reaction, every 5 min to 40 min, then every 20 min until the end of the reaction. In general, the samples were taken within 20 s.

2.4. Product analysis

The reaction species in the samples were methylated with 25% aqueous tetramethylammonium hydroxide (TMAH) solution (details in ASTM Standard D 5974-00) and quantitatively analyzed by gas chromatography (GC) on a Varian CP-3380 GC equipped with a fused silica capillary column coated with DB-5 (30 m × 0.25 mm i.d. × 0.25 μm film thickness, J&W Scientific, USA) and a flame ionization detector (FID). The operating conditions of the gas chromatography were as follows: (i) initial column temperature 423 K for 0 min, program at 4 K min^{-1} to 493 K, then at 2 K min^{-1} to 533 K; (ii) nitrogen, with a flow rate of 45 ml min^{-1}, was used as carrier gas; the pressure before the column was 0.07 MPa; the flow rate of air was 300 ml min^{-1}; (iii) the flow rate of hydrogen was 30 ml min^{-1} and (iv) the temperatures of the detector and injection ports were held at 533 K. Analysis was taken using a 1/50 split ratio. A 0.2 μl sample of the methylated reaction mixture was injected into the GC [13,17].

The reaction products were qualitatively analyzed by GC–MS method, using a system that coupled an HP model series 6890 gas chromatograph with an HP model 5973 mass selective detector (Agilent Technologies), using a silica column HP-5MS (30 m × 0.25 mm i.d. × 0.25 μm film thickness, Agilent, USA). The carrier gas was helium at a flow rate of 1.0 ml min^{-1} and the voltage of electron impact ionization was 70 eV.

2.5. The elimination of external and internal diffusion effects

Catalytic disproportionation of rosin over a Pd/C catalyst is a liquid–solid two-phase reaction. In order to determine the kinetic model in the absence of mass transfer effects, several preliminary runs were carried out to investigate the effects of internal and external diffusion [18].

The external diffusion is reflected in the rate at which the rosin reaches the surface of the catalyst. The resistance effect of external diffusion focuses on the viscous flow over the catalyst surface. The effect of external diffusion can be eliminated by changing the speed of the mechanical stirrer. This effect was investigated using a fixed amount of catalyst with the rosin at a reaction temperature of 553 K. Based upon the results in Fig. 2(a), the fixed amount of catalyst was chosen to be 0.1% (w/w). As shown in Fig. 2(b), the conversion increased with increased stirring speed, up to 400 rpm. Therefore, in the present investigation, the external diffusion effect was eliminated by using stirrer speeds above 500 rpm.

The absence of intraparticle mass transfer (i.e., internal diffusion) resistance was explored by studying the effect of catalyst particle size [19–21]. Experiments were performed with four particle sizes ranging from <40 μm to 140–160 μm at 553 K. As can be seen in Fig. 3, no differences in conversion were found for catalytic particle diameters below 60–80 μm. In the present experiment, the particle size of Pd/C catalyst is between 10 and 20 μm; hence, pore diffusion was deemed to be absent.

3. Results and discussion

3.1. Catalyst characterization

The basic characteristics of the 5% Pd/C are given in Table 1. The mean catalyst particle size of Pd/C was 16 μm. The SEM images of 5% Pd/C catalyst and the carbon support are shown in Fig. 4 and reveal that both the catalyst and support particles are irregular in shape. It is seen that the morphology of the catalyst before and after its preparation changes slightly resulting in slightly larger particles, as described in SEM images in Fig. 4(a and b). This can be attributed to catalyst preparation method, impregnation technique. Recently, Tike and Mahajani [15] and Wang et al. [22] have also observed analogous changes in the morphology of the support

Table 1
Basic characterizations of Pd/C catalyst.

Specific surface area BET (m^2 g^{-1})	927.4
Total pore volume (cm^3 g^{-1})	0.56
Average pore diameter (Å)	13.5

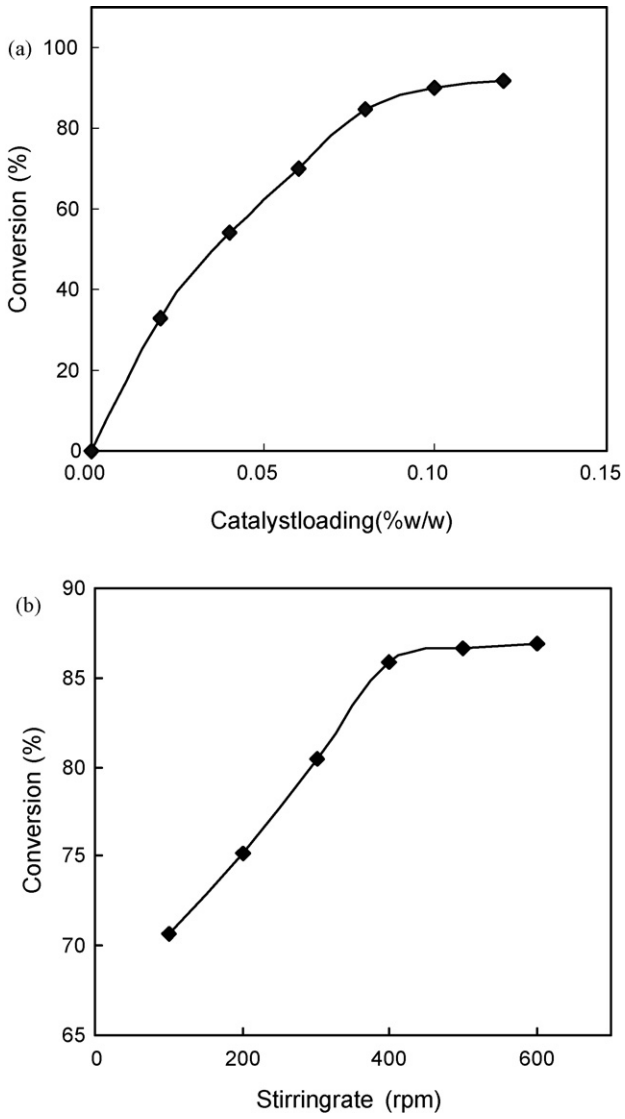

Fig. 2. (a) Effect of catalyst loading on the conversion of rosin acid (503 K, reaction time 120 min, stirring rate 500 rpm, rosin 420 g); (b) effect of stirrer rate on the conversion of rosin acid (553 K, reaction time 10 min, catalyst loading 0.1% (w/w) of rosin, rosin 420 g).

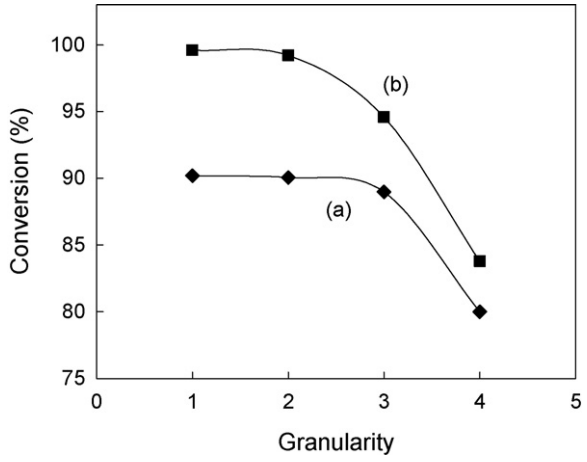

Fig. 3. Variation of the conversion of rosin acid with granularity of catalyst [granularity of catalyst: 1 (<40 μm); 2 (60–80 μm); 3 (100–120 μm); 4 (140–160 μm)] (a) 503 K, reaction time 120 min, stirring rate 500 rpm, catalyst loading 0.1% (w/w) of rosin, rosin 420 g and (b) 553 K, reaction time 30 min, stirring rate 500 rpm, catalyst loading 0.1% (w/w) of rosin, rosin 420 g.

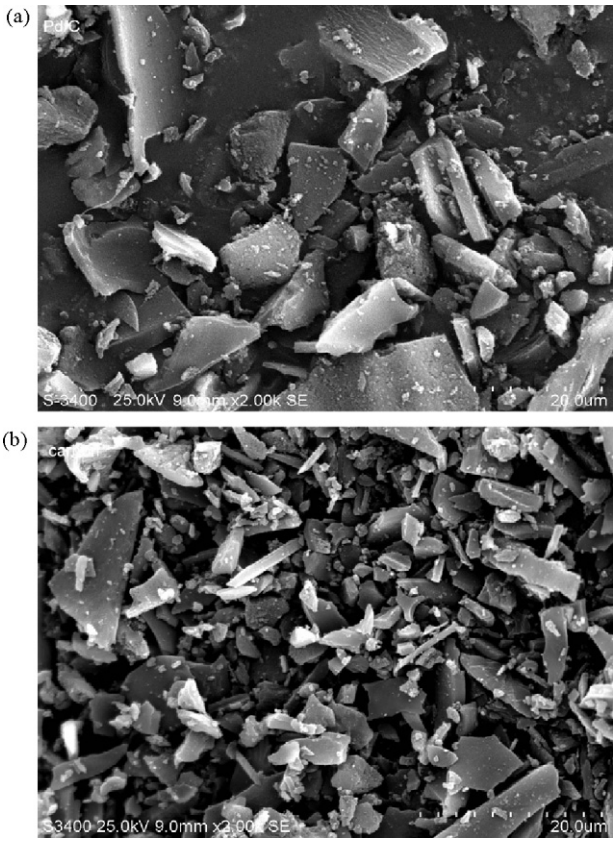

Fig. 4. Scanning electron micrograph of (a) 5% Pd/C catalyst and (b) carbon support.

during the preparation of a Pd-based catalyst used in the hydrogenation of soybean oil and of SiO_2-based catalyst used in the photo-catalytic degradation, in which impregnation technique of the catalyst preparation leads to the slight changes. According to SEM–EDS analysis, Pd/C catalyst contained 4.68 wt% of palladium.

The crystalline structure of the Pd/C catalyst was determined using XRD, and the result is shown in Fig. 5. It can be clearly seen that the sample exhibited four peaks at 2θ of 40.04°, 46.53°, 68.05° and 82.01°, ascribed respectively to (1 1 1), (2 0 0), (2 2 0) and (3 1 1) reflections of Pd metal with a facecentered cubic (fcc) structure. The XRD pattern shows a faintish signal to Pd, due to its high dispersion, which indicates the presence of Pd in small crystallites. The average size of the Pd crystallite particles was estimated from the full width at half maximum of the diffraction peaks to be 5.19 nm through Scherrer equation [23]. The metal dispersion of Pd/C is about 22%,

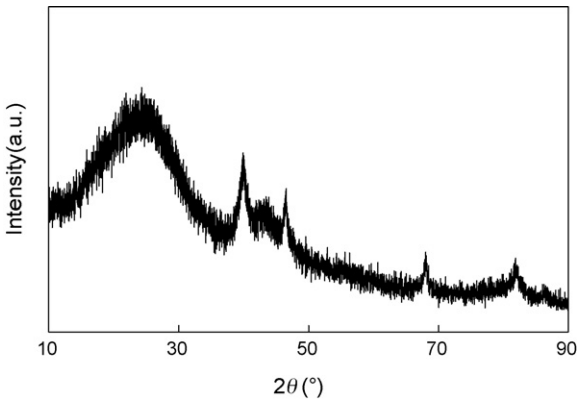

Fig. 5. X-ray diffraction pattern obtained for Pd/C catalyst.

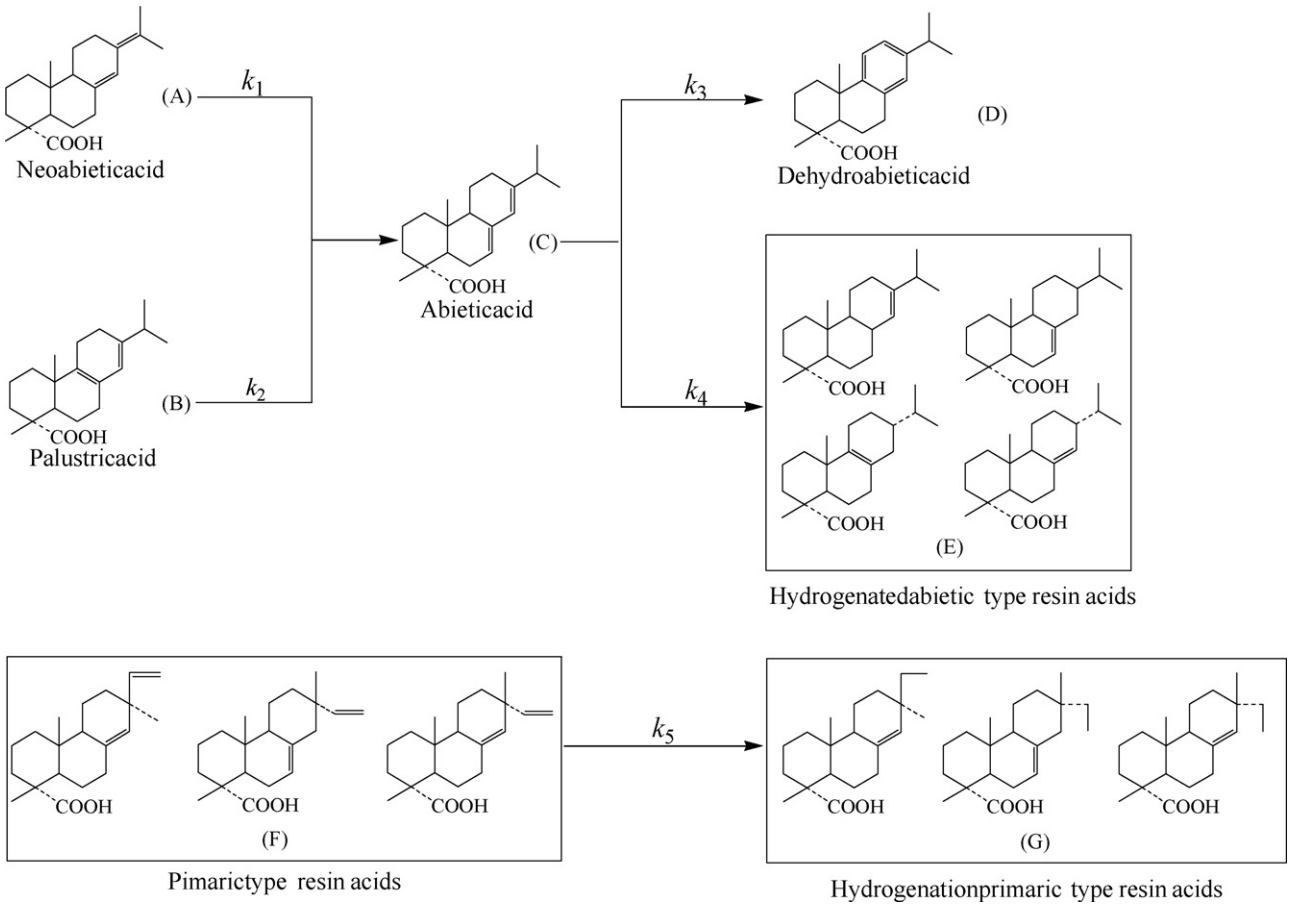

Fig. 6. The reaction network for catalytic isomerization and disproportionation of rosin over Pd/C catalyst.

calculated by the method of Pattabiraman and Fagherazzi et al. [24,25].

3.2. Reaction process analysis and kinetic model

Rosin disproportionation is generally understood to be an exchange of hydrogen among molecules of resin acids [6]. In the abietic-type resin acids, A represents the neoabietic acid, B is palustric acid, and C stands for abietic acid. The abietic-type resin acids can be easily isomerized by double bond rearrangement on heating, to form abietic acid that is stable to heat and acid [7]. Abietic acid, with conjugated double bonds, easily loses hydrogen atoms and then rearranges to form dehydroabietic acid (D represents dehydroabietic acid). The hydrogen atoms are transferred to other abietic acid molecules to form dihydroabietic acids. Similarly, pimaric-type resin acids, including pimaric acid and isopimaric acid, also accept hydrogen atoms to form hydrogenated pimarenoic acids. These reactions and rearrangements result in multiple isomers of dihydroabietic acids and hydrogenated pimarenoic type resin acids in the products [6,14].

In order to obtain a simple kinetic model for the isomerization and disproportionation reactions (see Fig. 6), according to the lumped method which has been successfully used in the complex kinetics of petroleum processing [26–31], the reaction species were divided into several lumps, based on similar structures. Here E represents hydrogenated abietic-type resin acids, F is pimaric-type resin acids and G is hydrogenated pimarenoic acid-type resin acids. In view of the above, the isomerization and disproportionation of the rosin resin acids can be described by scheme shown in Fig. 6, where k_1 is the rate constant for the isomerization of neoabietic acid to abietic acid (A → C); k_2 is the rate constant for the isomerization of palustric acid isomerization to abietic acid (B → C); k_3 is the rate constant for the dehydrogenation of abietic acid to dehydroabietic acid (C → D); k_4 is the rate constant for the hydrogenation of abietic acid to hydrogenated abietic-type resin acids (C → E) and k_5 is the rate constant for the hydrogenation of pimaric-type resin acids to hydrogenated pimarenoic acid-type resin acids (F → G).

In general, the models developed for describing the reaction with solid catalyst can be classified into two groups: pseudo-homogeneous and heterogeneous models. In the pseudo-homogeneous model, mass and heat transfers between the liquid and solid phases are negligible. Thus, the concentration of reactants and temperatures at catalyst surface are assumed to be the same as those in bulk phase whereas in the heterogeneous model, the difference of such state variables between different phases is taken into account. The aim of this work is to develop a simplified kinetic model of the catalytic isomerization and disproportionation of rosin over Pd/C catalyst. Under the condition that the diffusion effects have been eliminated, since the particle size of Pd/C catalyst used in our work is only between 10 and 20 μm and little catalyst loading, 0.1% (w/w) of reactant, a pseudo-homogeneous dynamic model for the liquid and solid phases can be assumed. And a first-order kinetic equation was assumed as well since the reactions just involve isomerization and exchange of hydrogen among molecules of rosin resin acids, which are merely double bond rearrangement of rosin resin acids molecules.

In this case, the reaction rate equation can be written as

$$\mathbf{R} = \frac{d\mathbf{c}}{dt} = \mathbf{k} \times \mathbf{c} \tag{1}$$

Table 2
Kinetic parameter for catalytic isomerization and disproportionation of rosin.

Kinetic constant	Temperature (K)						k_0 (min^{-1})	E_a (kJ mol^{-1})	ρ^2
	483	493	503	513	523	533			
k_1 (min^{-1})	0.0124 ± 0.0022	0.0252 ± 0.0014	0.0336 ± 0.0068	0.0796 ± 0.0225	0.2673 ± 0.1371	0.4212 ± 0.2132	7.92×10^{14}	156.14	0.968
k_2 (min^{-1})	0.0229 ± 0.0023	0.0338 ± 0.0012	0.0436 ± 0.0058	0.0603 ± 0.0116	0.0895 ± 0.0243	0.1588 ± 0.0392	7.14×10^{6}	78.80	0.977
k_3 (min^{-1})	0.0103 ± 0.0004	0.0167 ± 0.0002	0.0220 ± 0.0010	0.0413 ± 0.0022	0.0681 ± 0.0069	0.1367 ± 0.0126	5.00×10^{9}	108.56	0.980
k_4 (min^{-1})	0.0061 ± 0.0004	0.0103 ± 0.0002	0.0132 ± 0.0007	0.0270 ± 0.0017	0.0389 ± 0.0046	0.0768 ± 0.0077	1.54×10^{9}	105.75	0.982
k_5 (min^{-1})	0.0022 ± 0.0002	0.0038 ± 0.0005	0.0050 ± 0.0005	0.0089 ± 0.0013	0.0154 ± 0.0021	0.0201 ± 0.0036	7.27×10^{7}	97.35	0.990

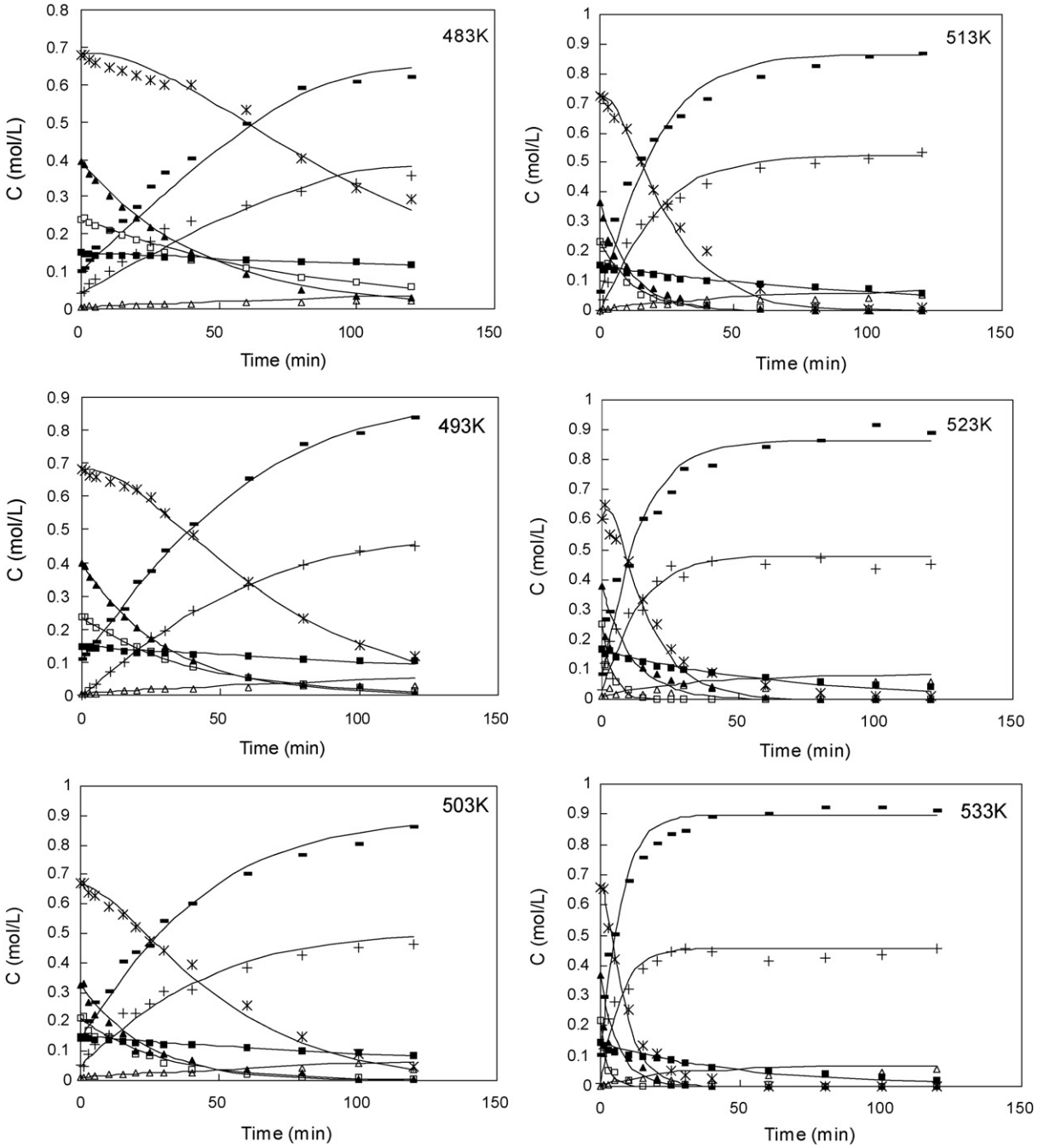

Fig. 7. A comparison of the experimental and calculated values of the concentrations of acids at different temperatures. Solid lines are calculated values and symbols are experimental values for neoabietic acid (□), palustric acid (▲), abietic acid (*), dehydroabietic acid (▬), hydrogenated abietic-type resin acids (+), and pimarenoic acid-type resin acids (■), hydrogenated pimarenoic acid-type resin acids (△).

where

$$\mathbf{R} = \left[\frac{dc_A}{dt} \quad \frac{dc_B}{dt} \quad \frac{dc_C}{dt} \quad \frac{dc_D}{dt} \quad \frac{dc_E}{dt} \quad \frac{dc_F}{dt} \quad \frac{dc_G}{dt} \right]$$

c_A, c_B, . . ., c_G represent the concentrations of the components and t refers to the observation times; $\mathbf{c} = [\, c_A \quad c_B \quad c_C \quad c_C \quad c_C \quad c_F \quad c_F \,]^{\mathrm{T}}$, $\mathbf{k}$ represents reaction rate constant matrix, expressed by:

$$\mathbf{k} = \begin{bmatrix} -k_1 & 0 & 0 & 0 & 0 & 0 & 0 \\ 0 & -k_2 & 0 & 0 & 0 & 0 & 0 \\ k_1 & k_2 & -(k_3+k_4) & 0 & 0 & 0 & 0 \\ 0 & 0 & 0 & k_3 & 0 & 0 & 0 \\ 0 & 0 & 0 & 0 & k_4 & 0 & 0 \\ 0 & 0 & 0 & 0 & 0 & -k_5 & 0 \\ 0 & 0 & 0 & 0 & 0 & 0 & k_5 \end{bmatrix} \quad (2)$$

The mass fraction of each composition was obtained by the quantitative analysis on gas chromatography. And then the mass fraction was converted into mole concentration through the mass balance equation as follows:

$$C_i = \frac{\omega_i \times G \times d}{M_i \times W} \times 1000 \quad (3)$$

where c is the concentration of compound, ω is the mass fraction, G is the mass of disproportionated rosin, d is the density of product liquid, M is the molecular weight, W is the mass of product liquid, i the component.

3.3. Modeling results

The rate constants were estimated using the Levenberg–Marquart nonlinear least-squares method [32], using a program written for the optimization in MATLAB [33]. The activation energies and frequency factors were then estimated using Statistical Program for Social Sciences (SPSS) software. In the parameter estimation routine the following objective function was minimized:

$$Q = \sum (c_i(t) - \hat{c}_i(t))^2 \quad (4)$$

where Q is the sum of the squares of the residuals (target function value); i refers to the component in the mixture; t refers to the observation time; c_i is the experimentally determined concentration of the ith component and $\hat{c}_i$ is the concentration of the ith component calculated from the rate equation matrix of the model.

The rate constants along with their limits of confidence interval at different temperatures were estimated based on 84 groups of data, and the results are presented in Table 2. A comparison between calculated and experimental values for the concentrations of each component at 483–533 K is given in Fig. 7. The points represent the measured concentrations and the solid lines represent the estimated ones.

The reaction rate constants in Table 2 were correlated with the Arrhenius equation after data linearizing:

$$K = k_0 \ \mathrm{e}^{-E_a/RT} \quad (5)$$

The activation energy (E_a) and frequency factor (k_0) of the various reactions were obtained using SPSS software, and the results are presented in Table 2. The high values for the linear correlation coefficient ρ^2 indicate a close match between the experimental and modeled data.

3.4. Discussion

The model describes the isomerization of neoabietic acid and palustric acid isomerize to abietic acid during the disproportionation of rosin over Pd/C catalyst. This isomerization also takes place in rosin by the action of heat or acids, but with the action of heat or acids the reaction does not continue to the formation of dehydroabietic acid and hydrogenated abietic-type resin acids; i.e., abietic acid reaches equilibrium with neoabietic acid and palustric acid. In the presence of the Pd/C catalyst, however, the abietic acid continues to dehydrogenate to dehydroabietic acid and hydrogenate to hydrogenated abietic-type resin acids. This continued reaction of the abietic acid would further promote the isomerization of neoabietic acid and palustric acid to abietic acid due to LeChatlier's Principle. Thus, in this view, the neoabietic acid and palustric acid do not simply disproportionate; rather, they initially isomerize to abietic acid, after which disproportionation occurs. This conclusion is similar to that reached in investigations of rosin polymerization [34,35].

The parameters in Table 2 show that the relationship between the various reaction rate constants at 483–533 K over Pd/C catalyst is k_1 or $k_2 > k_3 > k_4 > k_5$. Therefore, the rate of the isomerization of abietic-type resin acids can satisfy the demands for the disproportionation of abietic acid. Although dehydroabietic acid with its aryl structure and hydrogenated abietic-type acids with their alicyclic structures are all stable, the rate of abietic acid dehydrogenation (k_3) is greater than that of abietic acid hydrogenation (k_4), which is consistent with dehydroabietic acid forming the main constituent in the production of disproportionated rosin. Hence, the Pd/C catalyst possesses higher selectivity for dehydrogenation during the disproportionation of abietic acid. The reaction rate for the hydrogenation of abietic acid (k_4) is greater than that for pimarenoic acid-type resin acids (k_5), which is expected because abietic acid contains reactive conjugated double bonds. This also suggests that some of the hydrogen that is removed from the abietic acid is available for hydrogenation of the exocyclic vinyl group of the pimaric-type acids.

The data of E_a in Table 2 shows the activation energy of palustric acid isomerization is less than that of neoabietic acid isomerization during rosin disproportionation. Therefore, neoabietic acid isomerization becomes more important at higher temperature. The activation energy of abietic acid dehydrogenation is higher than the activation energy of abietic acid hydrogenation, which means dehydrogenation becomes more important among the competing reactions at higher temperature. Consequently, these data would predict that the reaction selectivity for dehydroabietic acid during rosin disproportionation can be improved if the reaction is carried out at higher temperatures.

3.5. Model examination

The experimental data for the disproportionation of rosin, in the temperature range 483–533 K fitted well to the calculations from the kinetic model as seen in Fig. 7.

A statistical F-test was performed at the 95% significance level to determine the significance of the results from the model. From the result in Table 2, it can be seen that all of the estimated parameters in the final optimization have a reasonable confidence interval indicating that the experiments for parameter estimation were sufficient. The results of statistics test are shown in Table 3. It can be seen that all the correlation coefficients (ρ^2), at various tempera-

Table 3
Results of statistical test for the model of rosin isomerization and disproportionation reaction.

Temperature (K)	ρ^2	Q	F
483	0.995	0.0448	660.48
493	0.998	0.00462	1085.14
503	0.996	0.0327	678.26
513	0.994	0.0592	433.98
523	0.986	0.146	170.09
533	0.993	0.0823	343.34

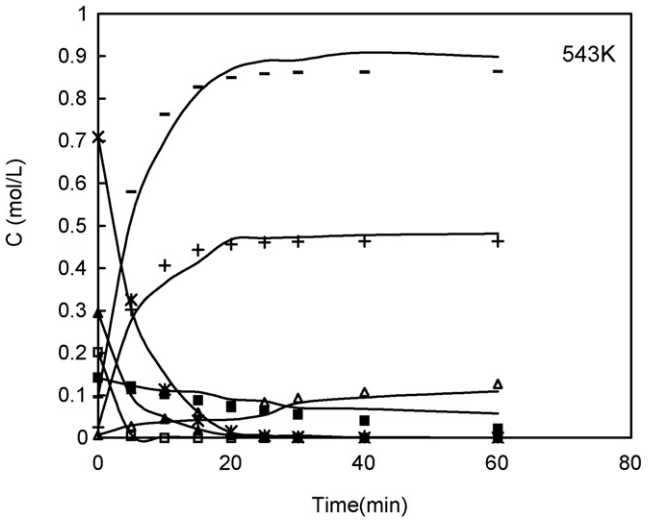

Fig. 8. Comparison between observed and calculated values of the concentrations of acids at 543 K. Solid lines are the calculated values and symbols are experimental values for neoabietic acid (□), palustric acid (▲), abietic acid (*), dehydroabietic acid (▬), hydrogenated abietic-type resin acids (+), and pimarenoic acid-type resin acids (■), hydrogenated pimarenoic acid-type resin acids (△).

tures, are over 0.90, and all of the calculated F values are greater than F_t value ($F_{0.05}$ (5, 9) = 3.48) multiplied 10, which was taken from the table. These results state that the kinetic model is significant within the 95% confidence level.

In order to test the predictive ability of the kinetic model and the reliability of the kinetic parameters, a rosin disproportionation experiment over a Pd/C catalyst was performed at temperature of 543 K. The comparison between the experimental and calculated values at 543 K is shown in Fig. 8. These data show that the proposed kinetic model can predict the concentration of each component in disproportionation of rosin at a temperature that is outside of the experimental range used to determine the model parameters.

4. Conclusions

The kinetics for the catalytic isomerization and disproportionation of rosin over Pd/C catalyst was studied. A novel experimental setup, with a double-tier paddle agitator and special sampling system that filters the sample and keeps it warm, has been developed for the study of the reaction kinetics, in a highly viscous liquid–solid reaction with readily crystallizing material under conditions of high temperature and pressure. Kinetic experiments in the absence of mass-transport limitation were carried out for 483–533 K, using a catalyst 0.1 wt% and a stirring rate of 500 rpm. A kinetic model for catalytic isomerization and disproportionation of rosin over a Pd/C catalyst was proposed. The kinetic parameters for each involved reaction were estimated using the Levenberg–Marquart method by MATLAB software. The proposed model meets the requirement of a F-test with 95% confidence level and provided a good simulation of the experimental kinetic data. Finally, the model was also shown to predict well the concentration distribution of the products from rosin disproportionation at 543 K.

Nomenclature

A	neoabietic acid
B	palustric acid
C	abietic acid
c	concentration (mol L^{-1})
D	dehydroabietic acid
d	density of product liquid (g cm^{-3})
E	hydrogenated abietic-type resin acids
E_a	activation energy (kJ mol^{-1})
F	pimaric-type resin acids
F	calculated values of F-test
F_t	tabled values of F-test
G	hydrogenated pimarenoic acid-type resin acids
k	rate constant for reaction (min^{-1})
k_0	frequency factor (min^{-1})
M	molecular mass (g mol^{-1})
Q	sum of square of residuals, target function value
r	reaction rate (mol min^{-1} L^{-1})
t	time (min)
W	mass of product liquid (g)
ρ^2	correlation coefficient of model
ω	mass fraction (%)

Acknowledgements

The authors gratefully acknowledge financial support for this research from the National Natural Science Foundation of China (30560119), the Doctorate Foundation of the State Education Ministry of China (20070593004) and the Scientific Research Foundation of Guangxi University (X081020). We also thank Prof. Liming Li for her valuable discussions and suggestions on implementing parameter estimation computer methods.

References

[1] H.I. Enos Jr., G.C. Harris, G.W. Hendrick, Rosin and rosin derivatives, in: A. Standen (Ed.), Kirk-Othmer Encyclopedia of Chemical Technology, vol. 17, second ed., Wiley, New York, 1968, pp. 475–508.
[2] H. Murai, K. Ohata, H. Enomoto, K. Sempuku, US Patent 4,210,671 (1980).
[3] T. Fonseca, B. Gigante, M.M. Marques, T.L. Gilchrist, E. De Clercq, Synthesis and antiviral evaluation of benzimidazoles, quinoxalines and indoles from dehydroabietic acid, Bioorgan. Med. Chem. 12 (1) (2004) 103–112.
[4] A.A. Tapia, M.D. Vallejo, S.C. Gouiric, G.E. Feresin, P.C. Rossomando, D.A. Bustos, Hydroxylation of dehydroabietic acid by *Fusarium* species, Phytochemistry 46 (1) (1997) 131–133.
[5] P.S. Piispanen, U.R.M. Kjellin, B. Hedman, T. Norin, Synthesis and surface measurements of surfactants derived from dehydroabietic acid, J. Surfactants Deterg. 6 (2) (2003) 125–130.
[6] Z.Q. Song, E. Zavarin, D.F. Zinkel, On the palladium-on-charcoal disproportionation of rosin, J. Wood Chem. Technol. 5 (4) (1985) 535–542.
[7] E. Stoltes, D.F. Zinkel, Chemistry of rosin, in: D.F. Zinkel, J. Russell (Eds.), Naval Stores: Production, Chemistry and Utilization, Pulp Chemicals Association, New York, 1989, pp. 261–345.
[8] E.E. Fleck, S. Palkin, US Patent 2,239,555 (1941).
[9] N.L. Kalman, US Patent 2,395,278 (1946).
[10] B.L. Hampton, US Patent 2,497,882 (1950).
[11] J.M.G. Correia, US Patent 4,659,513 (1987).
[12] J.Y. Jadhav, US Patent 6,087,318 (2000).
[13] V.M. Loeblich, R.V. Lawrence, Chromatographic investigation of disproportionated rosin, J. Am. Oil Chem. Soc. 33 (7) (1956) 320–322.
[14] Z.Q. Song, Z.Q. Liang, Study on reaction mechanism of disproportionation of Chinese gum rosin catalysed by palladium-on-charcoal, Chem. Ind. Forest Prod. 17 (3) (1997) 13–17 (in Chinese).
[15] M.A. Tike, V.V. Mahajani, Studies in catalytic transfer hydrogenation of soybean oil using ammonium formate as donor over 5% Pd/C catalyst, Chem. Eng. J. 123 (1–2) (2006) 31–41.
[16] A. Drelinkiewicz, A. Waksmundzka-Gora, Investigation of 2-ethylanthraquinone degradation on palladium catalysts, J. Mol. Catal. A: Chem. 246 (1–2) (2006) 167–175.
[17] L.L. Wang, X. Xu, X.P. Chen, W.J. Sun, Z.F. Tong, Characterization of the reaction products from pine gum catalytic disproportionation by gas chromatography/mass spectrometry, Chin. J. Chromatogr. 25 (3) (2007) 413–417 (in Chinese).
[18] V.R. Gangwal, J. van der Schaaf, B.F.M. Kuster, J.C. Schouten, The effect of mass transport limitation on the estimation of intrinsic kinetic parameters for negative order reactions, Appl. Catal. A: Gen. 274 (1–2) (2004) 275–283.
[19] R.J. Grau, P.D. Zgolicz, C. Gutierrez, H.A. Taher, Liquid phase hydrogenation, isomerization and dehydrogenation of limonene and derivatives with supported palladium catalysts, J. Mol. Catal. A: Chem. 148 (1–2) (1999) 203–214.
[20] A. Santos, P. Yustos, A. Quintanilla, F. Garcia-Ochoa, Kinetic model of wet oxidation of phenol at basic pH using a copper catalyst, Chem. Eng. Sci. 60 (17) (2005) 4866–4878.
[21] M.I. Cabrera, R.J. Grau, Liquid-phase hydrogenation of methyl oleate on a Ni/α-Al_2O_3 catalyst: a study based on kinetic models describing extreme and

intermediate adsorption regimes, J. Mol. Catal. A: Chem. 260 (1–2) (2006) 269–279.
[22] Y.P. Wang, P.Y. Peng, H.Y. Ding, Y. Wu, Preparation and catalytic activity of active-carbon-supported TiO_2, Acta Sci. Circumst. 25 (5) (2005) 611–617 (in Chinese).
[23] B.D. Cullity, Elements of X-Ray Diffraction, Addison-Wesley, New York, 1978.
[24] R. Pattabiraman, Electrochemical investigations on carbon supported palladium catalysts, Appl. Catal. A: Gen. 153 (1–2) (1997) 9–20.
[25] G. Fagherazzi, A. Benedetti, S. Polizzi, A. Di Mari, F. Pinna, M. Signoretto, N. Pernicone, Structural investigation on the stoichiometry of β-PdHx in Pd/SiO_2 catalysts as a function of metal dispersion, Catal. Lett. 32 (3–4) (1995) 293–303.
[26] A.G. Gayubo, P.L. Benito, A.T. Aguayo, M. Castilla, J. Bilbao, Kinetic model of the MTG process taking into account the catalyst deactivation. Reactor simulation, Chem. Eng. Sci. 51 (11) (1996) 3001–3006.
[27] V.K. Pareek, A.A. Adesina, A. Srivastava, R. Sharma, Sensitivity analysis of rate constants of Weekman's riser kinetics and evaluation of heat of cracking using CATCRAK, J. Mol. Catal. A: Chem. 181 (1–2) (2002) 263–274.
[28] J. Singh, M.M. Kumar, A.K. Saxena, S. Kumar, Reaction pathways and product yields in mild thermal cracking of vacuum residues: a multi-lump kinetic model, Chem. Eng. J. 108 (3) (2005) 239–248.
[29] X.H. Meng, C.M. Xu, J.S. Gao, L. Li, Catalytic pyrolysis of heavy oils: 8-lump kinetic model, Appl. Catal. A: Gen. 301 (1) (2006) 32–38.
[30] G.M. Bollas, A.A. Lappas, D.K. Iatridis, I.A. Vasalos, Five-lump kinetic model with selective catalyst deactivation for the prediction of the product selectivity in the fluid catalytic cracking process, Catal. Today 127 (1–4) (2007) 31–43.
[31] H.Q. Zhou, Y. Wang, F. Wei, D.Z. Wang, Z.W. Wang, Kinetics of the reactions of the light alkenes over SAPO-34, Appl. Catal. A: Gen. 348 (1) (2008) 135–141.
[32] D.W. Marquardt, An algorithm for least-squares estimation of non-linear parameters, J. Soc. Ind. Appl. Math. 11 (1) (1963) 431–441.
[33] A. Constantinides, N. Mostoufi, Numerical Methods for Chemical Engineers with MATLAB Applications, Prentice Hall, New Jersey, 1999.
[34] J.J. Jiang, K.R. Ye, K. Feng, Catalytic isomerization–dimerization of resin acids of rosin with HCl–$ZnCl_2$, Chem. Ind. Forest Prod. 9 (2) (1989) 17–27 (in Chinese).
[35] B.A. Parkin Jr., W.H. Schuller, Catalyst–solvent system for dimerization of abietic acid and rosin, Ind. Eng. Chem. Prod. Res. Dev. 11 (2) (1972) 156–158.